JOURNAL OF APPLIED ELECTROCHEMISTRY 15 (1985) 259–265

Electrochemical reduction of niobium ions in molten LiF–NaF

QIAO ZHIYU*, TAXIL PIERRE

Laboratoire de Chimie Physique et d'Electrochimie, CNRS LA 192, Université Paul Sabatier, 118 Route de Narbonne, 31062 Toulouse Cedex, France

Received 5 May 1984

The mechanism of the electrochemical reduction of niobium ions in molten LiF–NaF (1 : 1 mol) has been studied in detail at 750 and 800° C by the use of cyclic voltametry, chronoamperometry and chronopotentiometry. In the solution of niobium ions in LiF–NaF, it is concluded that the mechanism for the electrochemical reduction of fluoroniobate is:

$$Nb^{V} + e \rightarrow Nb^{IV}$$

$$Nb^{IV} + 4e \rightarrow Nb^{0}$$

at potentials of about − 0.06 and − 0.17 V, respectively (referred to the reliable Ni/NiF_2 (1 mol %) electrode [1]. The electrochemical reaction $Nb^{IV} + 4e \rightarrow Nb^{0}$ is a (quasi)reversible and diffusion-controlled process.

The conclusion has also been confirmed by analysis of the cathodic product obtained at constant potential with a scanning electron microscope.

1. Introduction

The mechanism of the electrochemical reduction of niobium ions in fluoride and fluoride–chloride molten salts has already been studied by several authors [2–10]. However, the results are different from each other. Starting from a solution of K_2NbF_7 in Flinak‡, Mellors and Senderoff [3] observed three reduction steps by means of chronopotentiometry:

$$Nb^{V} + e \rightarrow Nb^{IV} + 3e \rightarrow Nb^{I} + e \rightarrow Nb^{0} \qquad (1)$$

at potentials: − 0.11, − 0.76 and − 1.02 V. (referred to the Ni/NiF_2 electrode). In the usual tetravalent solution which was generated by the disproportionation of Nb^{V} as K_2NbF_7 and Nb metal in molten Flinak which is used for plating, only the last two steps occur. Yoko and Bailey [8] investigated the electrochemical behaviour of Nb^{V} in molten Flinak using the method of cyclic voltametry and chronopotentiometry and showed that Nb^{V} is reduced in two steps:

$$Nb^{V} + 2e \rightarrow Nb^{III} + 3e \rightarrow Nb^{0} \qquad (2)$$

In molten KCl–NaCl–K_2NbF_7 and in molten KCl–KF–K_2NbF_7 Chemla [9] and Konstantinov, Polyakov and Stangrit [10], respectively, found two steps of niobium reduction:

$$Nb^{V} + e \rightarrow Nb^{IV} + 4e \rightarrow Nb^{0} \qquad (3)$$

To aim at a better understanding of the mechanism of the electrochemical reduction of niobium ions, further study on the cathodic reduction of niobium ions in molten LiF–NaF (1 : 1 mol) at 750 and 800° C has been carried out by use of cyclic voltametry, chronoamperometry and chronopotentiometry.

2. Experimental details

2.1. *The electrochemical cell*

The electrolysis cell which was similar to that used for tantalum deposition is shown diagrammatically in Fig. 1. The details are described by Taxil and Mahenc [11].

*Permanent address: Beijing University of Iron and Steel Technology, Department of Physics and Chemistry of Metals, Beijing, China.

‡Flinak: eutectic melt LiF–NaF–KF.

0021–891X/85 $03.00 + .12

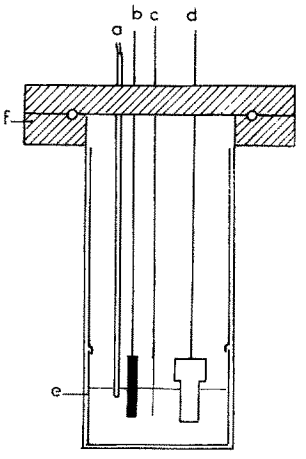

Fig. 1. Experimental device: (a) thermocouple, (b) counter electrode, (c) working electrode, (d) reference electrode, (e) nickel crucible, (f) stainless steel lid.

2.2. *Chemicals and salt preparation*

All the chemicals used are reagent grade.

LiF and NaF (Suprapur grade) were obtained from Merck Laboratory. The solute containing niobium, K_2NbF_7, and NiF_2 used in the reference electrode were obtained from Alpha Inorganics (purity: 99.9%). The reference electrode was isolated from the electrolyte by a sheet of boron nitride (Grade HP) provided by Carborundum. Molybdenum and nickel used as electrodes were purchased from Alpha Inorganics (purity 3 N) and graphite or vitreous carbon, used as counter electrode from Carbone Lorraine.

The LiF–NaF eutectic, with a freezing point of 650° C, was chosen as a suitable solvent from which solutions of K_2NbF_7 (from 5.85×10^{-5} to 1.46×10^{-4} mol %) were prepared. Each fluoride salt used was pure; after being well mixed and dried in an oven at 100° C for 24 h, the salt mixture was dehydrated in vacuum by slowly heating to the following temperatures and kept at these temperatures for 30 h each: 300 and 500° C. The bath was next melted under argon, then at 700° C argon gas was bubbled through it for 16 h. For the LiF–NaF eutectic alone the residual current at -1.2 V was 1.5 mA cm^{-2}. The K_2NbF_7 was dehydrated in vacuum at 350° C for 24 h. A solute assembly was used for the addition of K_2NbF_7 and niobium under argon atmosphere. In order to prepare a solution of fluoroniobate ions with niobium valence close to IV in NaF–LiF, excess niobium metal was added and a niobium anode was immersed in the melt to equilibrate the niobium

$$Nb + 4\ Nb^{V} \rightarrow 5\ Nb^{IV} \qquad (4)$$

at a value between 4.2 and 4.5 [2, 7].

2.3. *Electrodes*

The cathode was of 1 mm diameter pure molybdenum. Before use the molybdenum cathode was scoured in trichloroethene, then polished by electrolysis in a H_3PO_4–H_2SO_4 solution and finally washed with distilled water and acetone.

The counter electrode was made of 5 mm diameter pure graphite rod or 3 mm diameter vitreous carbon rod. These electrodes were washed with distilled water and acetone.

In the case of molten LiF–NaF–K_2NbF_7 the reliable Ni/NiF_2 ($X = 0.01$) electrode was used for the reference electrode. The stability, reproducibility and reversibility of the Ni/NiF_2 ($X = 0.01$) electrode was recently studied [1]. When in the molten solution the mean valence of niobium ions was approximately 4.5, the redox reference electrode Mo/Nb^{V}, Nb^{IV} was also used [1, 7]. The standard redox potential of this couple was -60 ± 5 mV at 750° C and -65 ± 5 mV at 800° C vs the Ni/NiF_2 ($X = 0.01$) reference electrode [1].

2.4. *Instrumentation*

A multipurpose installation was used based on a Tacussel PRT 20–10X potentiostat and a periodical triangular signal generator Tacussel Model GSTP 3. Cyclic voltamograms and chronopotentiograms were recorded with X–Y recorder and storage oscilloscope, Schlumberger 5071 or recorder Tacussel Type EPLI. Chronoamperograms were recorded on the same apparatus.

3. Results and discussion

3.1. *Cyclic voltametry*

A typical cyclic voltamogram of the molten LiF–NaF–K_2NbF_7 at 750° C on the molybdenum electrode is shown in Fig. 2. In the range of potential from + 0.2 to -1.2 V a second reduction wave at about -0.17 V is observed. However, the first reduction wave at about -0.06 V is not clear. But, according to the value of the standard redox

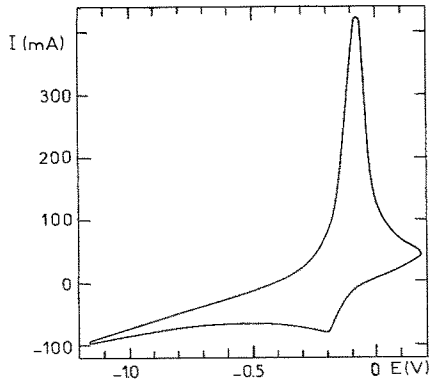

Fig. 2. Typical voltamogram of the molten LiF–NaF–K_2NbF_7 at 750° C with a Ni/NiF_2 ($x = 0.01$) reference electrode. ($X_{K_2NbF_7} = 5.85 \times 10^{-5}$ mol cm^{-3}, cathodic area, $A = 0.785$ cm^2, potential sweep rate $V = 0.056$ V s^{-1}.)

potential of the couple Nb^V/Nb^{IV}, one can reasonably consider that this step corresponds to the reduction of Nb^V to Nb^{IV} at about − 0.06 V and 750° C. It is obvious that the first and second successive reduction peaks occur too near each other to be separated.

In order to be sure that the second step corresponds to niobium deposition, in the case of niobium (V) and of approximately valence 4.5 the cathodic product obtained by electrolysis at constant potential from − 0.05 to − 0.25 V for 5 min was analysed by scanning electron microscopy with energy dispersive analysis of X-rays (Edax Model 711). Fig. 3 shows that in the case of electrolysis at a potential more positive than − 0.163 V only molybdenum was observed. However, at potentials from − 0.163 to − 0.25 V the niobium deposition on the molybdenum cathode surface was examined. It is certain that the second wave corresponds to niobium deposition.

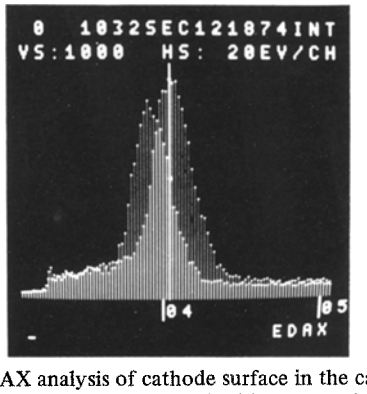

Fig. 3. EDAX analysis of cathode surface in the case of electrolysis at a potential which is: (a) more positive than − 0.163 V, when only molybdenum substrate (right peak) was observed; and (b) from − 0.163 to − 0.25 V, when niobium deposition (left peak) was also examined.

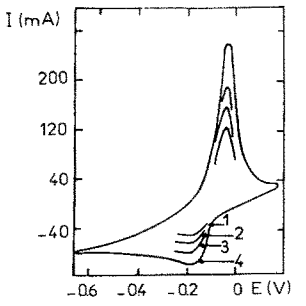

Fig. 4. Voltamograms of molten LiF–NaF–K_2NbF_7 at 750° C with a Ni/NiF_2 ($x = 0.01$) reference electrode ($X_{K_2NbF_7} = 5.85 \times 10^{-5}$ mol cm^{-3}, $A = 0.785$ cm^2 1 – 0.0112 V s^{-1}, 2 – 0.028 V s^{-1}, 3 – 0.043 V s^{-1}, 4 – 0.086 V s^{-1}.

According to the results of cyclic voltametry shown in Fig. 4, the peak potential of the second wave was independent of the potential sweep rate. It is clear that in Fig. 5 the cathodic current peak height is linear with the square root of the sweep rate.

The voltamogram of a solution of fluoroniobate ions with niobium valence of approximately 4.5 in NaF–LiF at 750° C is shown in Fig. 6. The process of electrochemical reduction is almost the same as that in molten LiF–NaF–K_2NbF_7. The peak potential of the second wave is independent of the potential sweep rate and the cathodic current peak height is also linear with the square root of the sweep rate.

It is obvious that in both cases the second reduction step of niobium ions corresponding to

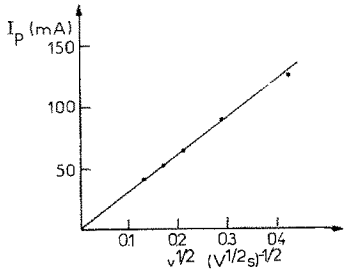

Fig. 5. A variation of the cathodic current peak height with the square root of the sweep rate ($X_{K_2NbF_7} = 5.85 \times 10^{-5}$ mol cm^{-3}, $A = 0.785$ cm^2, 750° C).

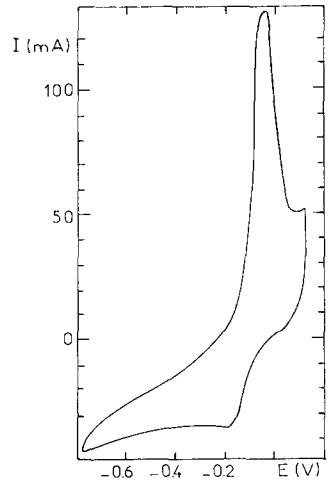

Fig. 6. Typical voltamogram of a solution of fluoroniobate ions with niobium valence of approximately 4.5 in NaF–LiF at 750° C with Ni/NiF_2 ($x = 0.01$) reference electrode ($X_{K_2NbF_7} = 1.46 \times 10^{-4}$ mol cm^{-3}, $A = 0.875$ cm^2, $V = 0.086$ V s^{-1}).

about -0.17 V is a simple (quasi)reversible charge transfer and diffusion-controlled process.

Since the separation between the first and the second wave is not great enough, the following equations can only be used for approximate estimation of the electron number involved in this step [12]:

$$E_{p/2} - E_p = 2.2RT/nF \quad (5)$$

$$E_{1/2} - E_p = 1.11RT/nF \quad (6)$$

or at 750° C

$$n = 0.1939/E_{p/2} - E_p \quad (7)$$

$$n = 0.0978/E_{1/2} - E_p \quad (8)$$

According to our experimental data, the difference between the half-peak potential, $E_{p/2}$, and the peak potential, E_p, as well as the difference between the potential corresponding to $0.85\,I_p$ [12] and E_p are:

$$E_{p/2} - E_p = 0.046\,\text{V} \quad (9)$$

$$E_{1/2} - E_p = 0.025\,\text{V} \quad (10)$$

Thus, the electron number, n, is calculated to be 4.2 and 3.9, respectively. Each is the average of five cyclic voltametric runs. This large value of n is in coordination with the shape of the i–E curve in Figs. 2, 4 and 6. Since n has a large effect upon the shape of the i–E curve, the sharp curve indicated that the value of n should be large.

The reason for the validity of Equations 5 and 6, which correspond to the case of reversible reduction of soluble matter, may be due to the change of the concentration at the electrode surface rather than the formation of surface alloy. One can assume that niobium crystallization on the electrode surface will react with Nb^V to produce Nb^{IV} according to the following reaction:

$$Nb + 4\,Nb^V \rightleftharpoons 5\,Nb^{IV} \quad (11)$$

Thus, the concentration of the reacting ion in the cathode surface is changed.

Thus one can consider that the cathodic process mechanism of niobium ions in the solution of fluoroniobate ions with niobium of valence 5 and approximately 4.5 in NaF–LiF is a double-step: $Nb^V + e \rightarrow Nb^{IV}$ and $Nb^{IV} + 4e \rightarrow Nb^0$ at potentials of about -0.06 and -0.17 V, respectively. This conclusion has been further confirmed by the results of chronoamperometry and chronopotentiometry.

3.2. *Chronoamperometry*

Further study on the deposition of niobium ions onto molybdenum electrode was made using chronoamperometry. Fig. 7 shows several current–time curves obtained with increasing applied potential. At potentials more positive than -0.156 V a typical diffusion-controlled transient is observed following the i–$t^{-1/2}$ relationship, that is, the Cottrell equation is obeyed.

$$it^{1/2} = nFAD^{1/2}C/\pi^{1/2} \quad (12)$$

It is clear that a process other than deposition

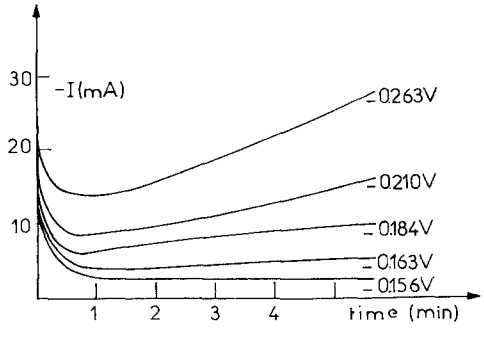

Fig. 7. Potentiostatic transients for the reduction of niobium ions in NaF–LiF–K_2NbF_7 at 800° C and at the applied potentials indicated ($A = 0.785$ cm^2).

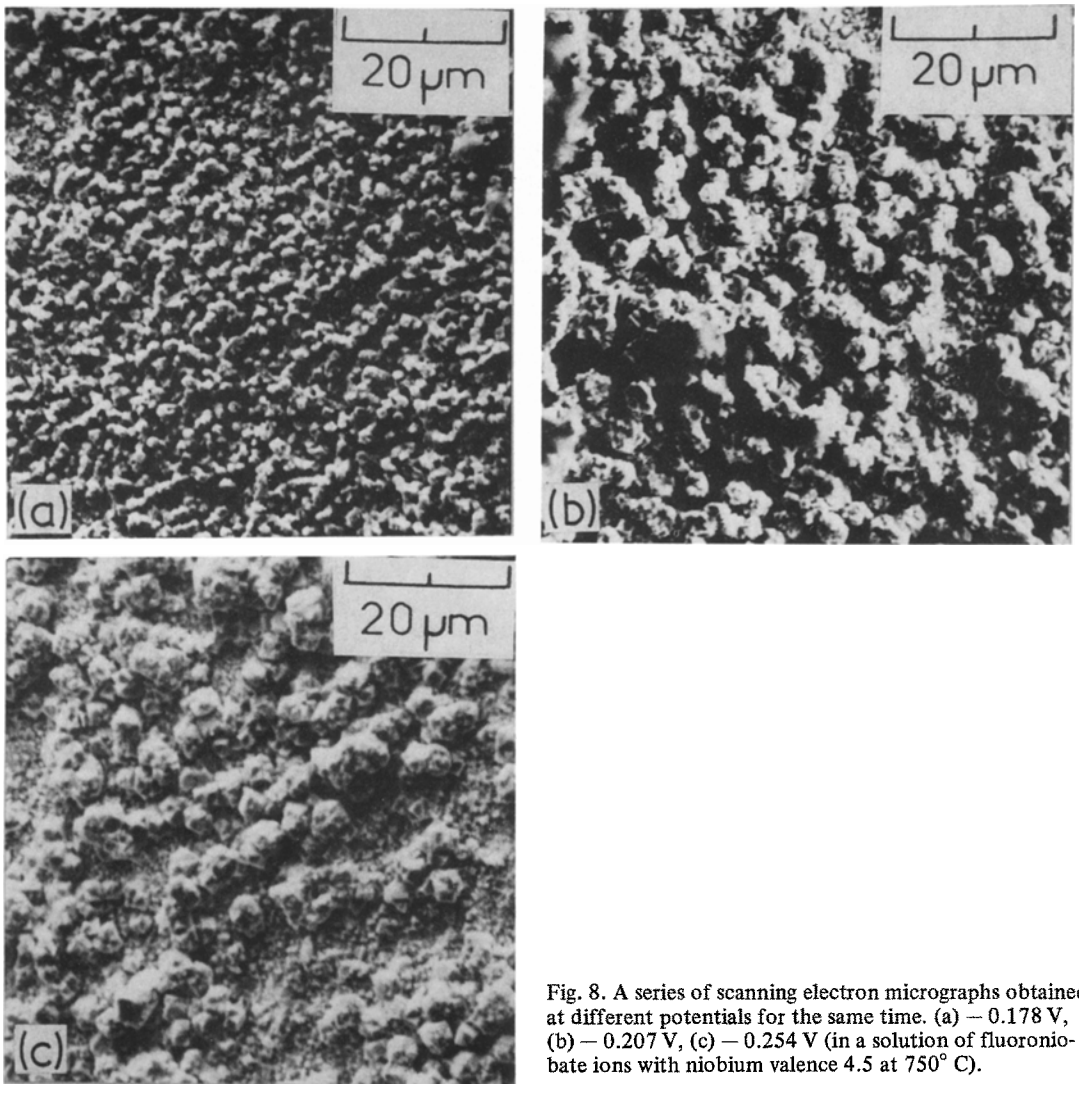

Fig. 8. A series of scanning electron micrographs obtained at different potentials for the same time. (a) − 0.178 V, (b) − 0.207 V, (c) − 0.254 V (in a solution of fluoroniobate ions with niobium valence 4.5 at 750° C).

occurs. At a potential more negative than − 0.156 V a significant change in the current–time transient occurs. After the initial double layer charging for some seconds, a minimum in the current occurs, followed by an increase of current. The minimum current and the time at which the minimum occurs are highly sensitive to the magnitude of the applied potential. The rising portion of the current–time curves obeyed the i–$t^{1/2}$ relationship approximately. Since the early stages of metal deposition are controlled by an instantaneous nucleation process [13, 14] and the current usually increases due to an increasing surface area and a change from planar to two- or three-dimensional diffusion [15], the minimum current and the i–$t^{1/2}$ relationship do show an instantaneous nucleation reaction. Just as shown in Fig. 3, at a potential of − 0.163 V and that more negative than − 0.163 V the niobium deposition on the molybdenum substrate was examined and nucleation as well as the growth process was found to occur.

Thus, it is concluded that the cathodic process mechanism of niobium ions mentioned above is reasonable. From Fig. 7 it is also shown that the extent and rate of nucleation and growth of niobium deposition are very sensitive to the value of the applied potential. This conclusion was confirmed by scanning electron microscopic examination of the molybdenum cathode surface. Figs. 8a–c show a series of photomicrographs obtained at different potentials for the same

time. Progressive stages of the growth of the niobium deposition were observed. The greater the extent of the niobium deposition, the more negative the applied potential for the niobium deposition to occur. The series of photomicrographs in combination with the potentiostatic transients in Fig. 7 also confirmed that the grain size increased with increasingly negative applied potential when the electrode reaction was controlled by the diffusion process which brings about dendrite formation [16]. Different techniques can be used to avoid dendrite formation. The periodic reversal (PR) technique, in which a cathodic (depositing) step is followed by an anodic (polishing) step was especially beneficial to the increase of plating rate of coherent niobium [6].

3.3. *Chronopotentiometry*

Typical chronopotentiograms are shown in Figs. 9 and 10. In both cases the first reduction wave is not observed. For the second reduction wave, the potential measured at a quarter of the cathodic transition time $E_{\tau/4}$ was independent of I: the value of $E_{\tau/4}$ was about -0.17 V. Assuming that the transition time of the first step, τ_1, is much smaller than that of the second step, τ_2 (at -0.17 V), they will be treated together just as Mellors and Senderoff [3] did, so that $\tau = \tau_1 + \tau_2$. Since by assuming $\tau_1 \ll \tau_2$, one can consider that this combined step is a reversible diffusion-controlled process. One may calculate n_2, the electron number of the second step from:

$$E = E_{1/2} + \frac{2.303RT}{n_2F} \log \left(\frac{\tau^{1/2} - t^{1/2}}{t^{1/2}} \right) \quad (13)$$

where t is any time up to the transition time τ, or the time corresponding to the length of the plateau in the chronopotentiogram. According to the data taken from Figs. 9 and 10 a plot of potential E vs $\log [(\tau^{1/2} - t^{1/2})/t^{1/2}]$ yielded a straight line with a slope of $2.303RT/nF$. The electron number n_2 corresponding to the second reduction wave was approximately 4.

Just as shown by the method of chronoamperometry and scanning electron microscopy, the second wave corresponds to the niobium deposition step. Thus, the sum of $n_1 + n_2 = 5$. Since n_2 has already been shown to be 4, n_1 must be unity. According to the chronopotentiogram of the molten LiF–NaF–K_2NbF_7 at 750° C (Fig. 9), the transition time τ_2 equals *c.* 2.15 s. On the basis of Equation 14, τ_1 equals about 0.09 s.

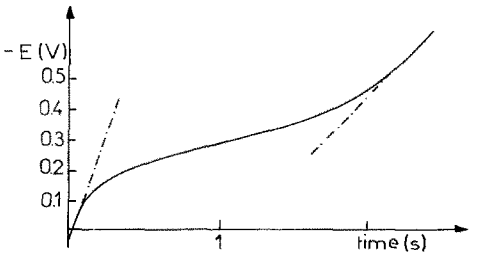

Fig. 9. Chronopotentiogram of molten LiF–NaF–K_2NbF_7 at 750° C with a Ni/NiF_2 ($x = 0.01$) reference electrode ($X_{K_2NbF_7} = 1.1 \times 10^{-4}$ mol cm^{-3}, $A = 0.785$ cm^2, $I =$ 90 mA).

$$\frac{\tau_2}{\tau_1} = \left(\frac{n_2}{n_1} \right)^2 + \frac{n_2}{n_1} \quad (14)$$

It is shown that the assumption of $\tau_1 \ll \tau_2$ is reasonable.

The stepwise reduction of a substance O according to the equations:

$$O + n_1 e = R_1 \quad (15)$$

$$R_1 + n_2 e = R_2 \quad (16)$$

has been treated by Berzins and Delahay [17]. In the case of electrochemical equilibrium the equation for the potential–time curve for the second step of the electrode process (Reaction 16) is as follows.

$$E = (E_{1/2})_{R_1 - R_2} + \frac{2.303RT}{n_2F} \times \log \frac{(\tau_1 + \tau_2)^{1/2} - (\tau_1 + t')^{1/2}}{(\tau_1 + t')^{1/2} - \tau_1^{1/2}} \quad (17)$$

where the potential $(E_{1/2})_{R_1 - R_2}$ is defined in the same fashion as the potential $E_{1/2}$ for the system O–R_1, that is, $(E_{1/2})_{R_1 - R_2}$ for Reaction 16 is determined experimentally at a time equal to $1/4\tau_2$. Besides, $\tau = \tau_1 + \tau_2$ and $t' = t - \tau_1$, t being the time elapsed since the beginning of the electrolysis (first step). Obviously, in the case of $\tau_1 \ll \tau_2$, one can neglect τ_1 and use the plot of potential E vs $\log [(\tau^{1/2} - t^{1/2})/t^{1/2}]$ to find the electron number n_2. The value is the same as that obtained above.

Thus, it is also confirmed that the conclusion

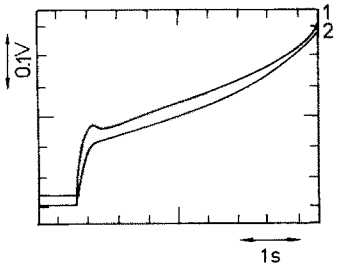

Fig. 10. Chronopotentiograms of a solution of fluoroniobate ions with niobium valence of approximately 4.5 in NaF–LiF at 750° C: 1 – on a clean molybdenum electrode, and 2 – a second pulse 1.5 min after 1 ($X_{K_2NbF_7} = 1.46 \times 10^{-4}$ mol cm^{-3}, $A = 0.785$ cm^2, $I = 80$ mA).

of a double-step mechanism obtained by use of cyclic voltametry and chronoamperometry is reasonable.

Comparing Curve 1 with Curve 2 of Fig. 10, a nucleation process is observed. The chronopotentiogram of Curve 1 is relative to a molybdenum electrode (which was polished by electrolysis before use) without initial nuclei. The chronopotentiogram of Curve 2 is relative to the next pulse applied on the same electrode without dissolving the niobium deposit. It is further certain that the reduction wave at $E_{1/4} = -0.17$ V corresponds to niobium deposition and the nucleation process is the early stage of metal deposition as has already been pointed out by several authors [13, 14, 18, 19].

4. Concluding remarks

Based on the experimental data obtained by use of cyclic voltametry, chronoamperometry, chronopotentiometry as well as scanning electron microscopy a double-step mechanism is proposed for the electrochemical reduction of niobium ions both in molten LiF–NaF–K_2NbF_7 and in a solution of fluoroniobate ions with niobium valence of 4.5 in NaF–LiF at 750 and 800° C. In both cases reduction can be considered to proceed according to the following scheme: $Nb^V + e \rightarrow Nb^{IV}$ and $Nb^{VI} + 4e \rightarrow Nb^0$ at potentials of about -0.06 and -0.17 V, respectively. The electrochemical reaction $Nb^{IV} + 4e \rightarrow Nb^0$ is (quasi)reversible and diffusion controlled.

The study also showed that the early stages of metal deposition are controlled by an instantaneous nucleation process and the grain size increased with the more negative potential applied when the electrode reaction was controlled by the diffusion process.

Acknowledgement

The authors are grateful to M. M. Victor, Daste, Perie (ENSAE, Department of Metallurgy) for EDAX analysis and SEM micrographs and to Professor M. Comtat for helpful discussion.

References

[1] P. Taxil and Qiao Zhiyu, to be published.
[2] G. W. Mellors and S. Senderoff, *J. Electrochem. Soc.* **112** (1965) 266.
[3] *Idem, ibid.* **113** (1966) 66.
[4] D. Inman and S. H. White, *J. Appl. Electrochem.* 8 (1978) 375.
[5] Y. Hirabayashi and I. Nakagawa, *Nagoya Kogyo Gijutsu Shikensho Hokoku* **30** (1981) 100.
[6] U. Cohen, *J. Electrochem. Soc.* **128** (1981) 731.
[7] *Idem*, PhD dissertation, Stanford University (1977).
[8] T. Yoko and R. A. Bailey, Proceedings of the First International Symposium on Molten Salt Chemistry and Technology, 20–22 April, 1983, Kyoto, Japan, p. 111.
[9] M. Chemla and V. Grinevitch, *Bull. Soc. Chim.* (1973) 853.
[10] V. I. Konstantinov, E. G. Polyakov and P. T. Stangrit, *Electrochim. Acta* **23** (1978) 713.
[11] P. Taxil and J. Mahenc, *Corros. Sci.* **21** (1981) 31.
[12] R. S. Nicholson and I. Shain, *Anal. Chem.* **36** (1964) 706.
[13] G. J. Hills, D. J. Schiffrin and J. Thompson, *Electrochim. Acta* 19 (1974) 657.
[14] G. A. Gunanardena, G. J. Hills, I. Montenegro and B. Scharifker, *J. Electroanal. Chem. Interfac. Electrochem.* **138** (1982) 225.
[15] K. L. Carleton, J. M. Olson and A. Kibbler, *J. Electrochem. Soc.* **130** (1983) 782.
[16] K. I. Popov, M. D. Maksimovic, I. D. Trajaneev and M. G. Pavlovic, *J. Appl. Electrochem.* **11** (1981) 239.
[17] T. Berzins and P. Delahay, *J. Amer. Chem. Soc.* 75 (1953) 4205.
[18] V. M. Rudoi, V. N. Samoilenko, E. V. Kandsler and A. I. Levin, *Electrokhim.* **11** (1975) 566.
[19] F. Lantelme, J. P. Hanselin and M. Chemla, *J. Electroanal. Chem.* 97 (1979) 49.